

Comparison of Rotational Energies and Rigidity of OCS-paraH₂ and OCS-⁴He complexes

R. E. Zillich and K. B. Whaley

Department of Chemistry and Pitzer Center for Theoretical Chemistry, University of California, Berkeley, CA 94720

Abstract

We analyze the nature of the rotational energy level structure of the OCS-He and OCS-H₂ complexes with a comparison of exact calculations to several different dynamical approximations. We compare with the clamped coordinate quasiadiabatic approximation that introduces an effective potential for each asymmetric rotor level, with an effective rotation Hamiltonian constructed from ground state averages of the inverse of the inertial matrix, and investigate the usefulness of the Eckart condition to decouple rotations and vibrations of these weakly bound complexes between linear OCS and ⁴He or H₂. Comparison with exact results allows an assessment of the accuracies of the different approximate methods and indicates which approaches are suitable for larger clusters of OCS with ⁴He and with H₂. We find the OCS-H₂ complex is considerably more rigid than the OCS-He complex, suggesting that semi-rigid models are useful for analysis of larger clusters of H₂ with OCS.

Key words:

PACS: 05.10.Ln, 33.20.Bx, 33.20.Ea, 34.30.+h, 36.40.-c

1 Introduction

Until recently, Helium-4 has been the only known boson superfluid liquid. Many aspects of superfluidity have been studied experimentally, phenomenologically, and theoretically. These include its relation to Bose-Einstein condensation, the temperature dependence of the superfluid fraction in the 2-fluid model, the finite size-dependence and the influence of atomic and molecular impurities in ⁴He on the superfluid fraction. The latter two issues have raised new, interesting and more basic questions. In particular, what is the validity

of phenomenological models on a microscopic scale, and how should we detect superfluidity of small systems. These questions ultimately demand a full microscopic understanding of superfluidity.

Rovibrational IR spectroscopy experiments with chromophores in helium droplets [1,2] have confirmed superfluid behavior for systems as small as approximately 60 ^4He atoms [3] by observing the free rotation of the OCS molecule. Subsequently, a new field of research has been opened by similar experiments in small para-hydrogen clusters embedded in low temperature helium droplets.[4] Spectroscopic experiments on OCS in these hydrogen clusters show spectroscopic anomalies which have been interpreted as indicating the existence of superfluidity of para- H_2 for clusters small enough to be fluid-like rather than forming a solid shell around the chromophore. These conclusions have recently been verified by path integral calculations showing that an anisotropic superfluid fraction appears at low temperatures ($T < 0.3$ K).[5] In addition, new experimental studies on very small complexes with less than one solvation shell of ^4He or H_2 obtained rotational/rovibrational excitation energies for complexes of well-defined size, OCS-pH_2 and $\text{OCS-}^4\text{He}_N$, $N = 1, \dots, 8$. [6,7,8,9,10] New theoretical work for small $\text{OCS-}^4\text{He}_N$ complexes [11] show an interesting transition from semi-rigid rotation of the whole cluster for small N to partial decoupling of the ^4He motion and the OCS rotation for increasing N . As explained in detail in Ref. [11], this implies a transition from a molecular complex to quantum solvation.

Quantitative microscopic calculation of the spectrum of excitation energies of $\text{OCS-(pH}_2)_N$ and $\text{OCS-}^4\text{He}_N$ clusters is an important step towards the understanding of the rovibrational spectra of these unusual clusters. For $N \gg 1$, this is still an extremely demanding task with current methodological and computational capabilities. Exact excitation energies are often not accessible and it is therefore necessary to make use of dynamical approximations, based whenever possible on existing knowledge of *e.g.* small cluster structures or on microscopic understanding of quantum solvation structures. In this paper, we therefore present a survey of approximate methods for the calculation of rotational energies of small Van der Waal complexes that have potential application to large quantum clusters of OCS in ^4He and in H_2 . In order to be able to critically assess the various approximations by comparing with exact results, we focus here on the smallest case, $N = 1$.

The methods we employ here are all based on diffusion Monte Carlo (DMC) sampling. Our focus on DMC methods derives from their suitability for application to larger sizes that are beyond the scope of basis set approaches. DMC yields exact results for ground state energies and the approximations employed here all take advantage of this. The approximate methods all assume some degree of rigidity, an assumption which we expect would progressively fail to be justified as one would go to larger clusters, with helium failing at

smaller cluster size than hydrogen. In section 3 we give an overview of how to calculate approximate rotational excitations. We described the clamped coordinate quasiadiabatic approximation of Quack and Suhm [12], a modification of it which incorporates the Eckart condition [13] for semi-rigid complexes, and a perturbative calculation of rotational constants following Ref. [14]. In section 4, we compare these results with the exact bound state energies determined by the program BOUND [15]. We discuss here also the relative rigidity of the OCS-He and OCS-H₂ systems as apparent from the grouping of exact energy levels into (ro)vibrational and rotational subsets, where “vibrational” from now refers to the radial motion of H₂ or ⁴He with respect to OCS. Section 5 summarizes and provides conclusions.

2 Ground state

The dimers OCS-pH₂ and OCS-⁴He are weakly bound van der Waals complexes which demand a full quantum mechanical calculation of the ⁴He degrees of freedom, due to their large zero-point motion. Exact methods [16,17,15] are available to determine ground and excited states of the dimers. However, we are interested in larger clusters OCS-(H₂)_N and OCS-⁴He_N, with special focus on the influence of the superfluid properties of the solvation shell around OCS [18,19]. For this reason, in this paper we employ diffusion Monte Carlo (DMC) which is applicable to large systems of sizes on the order of $N = 100$, and compare with the result of exact calculations for $N = 1$.

The theory and implementation of DMC has been described extensively in the literature [20,21,22]. We employ here a mixed branching-weighting algorithm. Reliable interaction potentials V between OCS and ⁴He, and H₂ (assumed spherical), respectively, have been calculated by Higgins *et.al.* [6,23]. Additional interaction potentials are available for the OCS-He system [24,25]. Fig. 1 shows cuts of the OCS-H₂ and two OCS-He potentials along the minimum energy path. In order to minimize computational cost in DMC, all potentials were expanded in Legendre polynomials and the resulting expansion coefficients interpolated with splines. This is responsible for the small irregularities in the lower panel of Fig. 1, but we have verified that these do not affect our results. In this work we will not be concerned with the determination and quality of the potentials in regard to experimental measurements, and shall therefore start our investigation with the given Hamiltonian

$$H = -\frac{\hbar^2}{2m_X}\nabla_X^2 - \frac{\hbar^2}{2M}\nabla_0^2 - B\left(\frac{\partial^2}{\partial\varphi_x^2} + \frac{\partial^2}{\partial\varphi_y^2}\right) + V(|\mathbf{r}_X - \mathbf{r}_0|, \cos\theta), \quad (1)$$

where $m_X = m(\text{H}_2)$ and $m(^4\text{He})$, B is the rotational constant of free OCS in

its ground state, and M its mass. $\partial\varphi_x$ and $\partial\varphi_y$ are the infinitesimal angles of rotation of the principal axis frame of OCS, $r \equiv |\mathbf{r}_X - \mathbf{r}_0|$ is the distance between atom and center of mass of OCS, and θ the angle between the OCS axis and the location of the atom. We employ the rigid body diffusion Monte Carlo algorithm[26,27] in which the rotational degrees of freedom φ_x and φ_y are sampled by random walks in the angular variable taken in the principal axis frame of the molecule. Although it is not essential for a system of only 8 coordinates $(\mathbf{r}_X, \mathbf{r}_0, \varphi_x, \varphi_y)$, of which only r and $u \equiv \cos\theta$ enter in the potential calculation, we employ biased DMC here, sampling the state $\Phi_0\Phi_T$ instead of Φ_0 , with the trial wave function

$$\Phi_T(r, u) = \exp \left[a_1 r^\alpha + (t_1 + \eta_1(u - u_1)^2) \log \frac{r}{a_2} + (t_2 + \eta_2 r^2(u - u_2)^2) e^{\eta - cr} \right] \quad (2)$$

which is flexible enough also for $N > 1$ complexes. The parameters of Φ_T are chosen to approximately minimize the energy expectation value, and are given in table 1. This trial function has both angular and radial dependence, and thus it requires the full rotational importance sampled algorithm developed in Ref. [27]. Importance-sampled DMC yields exact values for the ground state energy and also for expectation values of operators commuting with the Hamiltonian. Unless otherwise specified, all expectation values of operators not commuting with the Hamiltonian are computed here with descendent weighting [28] implemented according to the procedure for pure estimator of Ref. [29]. This corrects the mixed expectation values that result from importance sampling (*i.e.*, averages over the product $\Phi_0\Phi_T$) by a factor of Φ_0/Φ_T to obtain the exact expectation value over Φ_0^2 . This is particularly important for structural quantities.

3 Methods for Rotational excitations

Since DMC transforms the Schrödinger equation to a diffusion equation whose asymptotic solution is the ground state, DMC is often very efficient for the calculation of ground state properties while imposing only a small well controllable time step bias. The situation is quite different for excited states. Exact calculation of excitation energies is possible with the projection operation imaginary time spectral evolution approach (POITSE) which is generally very time-consuming.[30,31] Alternatively, excited states can be calculated with fixed node approximations, but these generally introduce an unknown amount of bias by the choice of nodal surfaces[31]. The methods described below share the element of approximation with fixed node in the sense that they are approximative, but possess the advantage that it is very straightfor-

ward and can be implemented with the same efficiency as ground state energy calculations.

3.1 Clamped coordinate quasiadiabatic approximation (ccQA)

We summarize here the procedure which Quack and Suhm [12] introduced to calculate rotational levels of the van der Waals dimer $(\text{HF})_2$. The rigid-rotor Hamiltonian H_{rot} of the instantaneous configuration \mathbf{R} at diffusion time t is obtained by diagonalizing the associated instantaneous inertial tensor I . For OCS- X_N , its elements in the body fixed frame of OCS are

$$I_{\alpha\beta} = \frac{\hbar^2}{2B}(\delta_{\alpha,\beta} - \delta_{\alpha,3}\delta_{\beta,3}) + \sum_i m_i(\delta_{\alpha,\beta}r_i - x_i^\alpha x_i^\beta)$$

with $r_i = \sum_\gamma x_i^\gamma x_i^\gamma$. Diagonalization yields principal values I_A , I_B , and I_C , and hence the rotational constants $A = \hbar/8\pi^2cI_A$, $B = \hbar/8\pi^2cI_B$, $C = \hbar/8\pi^2cI_C$. For $N = 1$ these should correspond to those of an asymmetric top for both He and H_2 complexes, as seen experimentally [7,8]. For given total angular momentum J , the resulting rigid-rotor cluster Hamiltonian is

$$H_{\text{rot}} = AJ_x^2 + BJ_y^2 + CJ_z^2. \quad (3)$$

This is diagonalized in a symmetric rotor basis,[32] resulting in eigenenergies $\epsilon_{J,\tau}$, $\tau = -J, \dots, J$. Since H_{rot} depends parametrically on the configuration \mathbf{R} , the energies $\epsilon_{J,\tau}$ are also parametrically dependent on \mathbf{R} . As pointed out by Quack and Suhm in Ref. [12], they can therefore be regarded as providing effective centrifugal potentials, $V_{J,\tau}(\mathbf{R}) = \epsilon_{J,\tau}$, which may be added to the cluster Hamiltonian (1) to yield an effective Hamiltonian for different rotational states of the cluster as a whole:

$$H_{J,\tau}(\mathbf{R}) = H(\mathbf{R}) + V_{J,\tau}(\mathbf{R}). \quad (4)$$

Because the Hamiltonians $H(\mathbf{R})$ and $H_{J,\tau}(\mathbf{R})$ differ only by the centrifugal potential terms, implementation of correlated sampling [33,34] on all systems $H_{J,\tau}(\mathbf{R})$ with a single random walk, but employing different individual weights is comparatively straightforward. Each system results in an excitation energy $E_{J,\tau}$, where these are the ground state energies of the respective effective Hamiltonians. The ground state energy E_0 can be calculated inexpensively together with all excitation energies $E_{J,\tau}$ in the single DMC run.

3.2 Eckart frame ccQA (EccQA)

The diagonalization of the moment of inertia tensor I at every (imaginary time) instant t amounts to choosing the principal axis of I as the instantaneous molecule fixed axis system, which thus moves with the motion of the generalized coordinate \mathbf{R} . However, the axis system which separates rotational and small vibrational motion most effectively is the Eckart frame [13] and this is the preferred axis system for the derivation of rovibrational Hamiltonians. Therefore, we modify the above ccQA prescription in the following manner to accommodate the preferred Eckart reference frame.

- (1) Instead of diagonalizing the instantaneous inertial tensor I (which is of course independent of the axis system used), we calculate the components $I_{i,j}$ in the Eckart frame and invert this matrix.
- (2) Instead of solving for the eigenvalues of the asymmetric top Hamiltonian (3), we solve for the eigenvalues $\epsilon_{J,\tau}$ of

$$H_{\text{rot}} = \sum_{i,j} (I^{-1})_{i,j} \hat{J}_i \hat{J}_j$$

This Hamiltonian is also used in the method described in the next section.

For the determination of the instantaneous Eckart frame, a reference geometry needs to be specified. In the case of OCS-X, it can be specified by the position of X with respect to the OCS center of mass and molecular axis, r_{ref} and $\cos \theta_{\text{ref}}$. As reference values of these coordinates, we choose the ground state expectation values $r_{\text{ref}} = \langle r \rangle$ and $\cos \theta_{\text{ref}} = \langle \cos \theta \rangle$. For OCS-H₂ and OCS-⁴He we find these expectation values are given by $r_{\text{ref}} = 3.704\text{\AA}$ and 3.935\AA , and $\theta_{\text{ref}} = 105.7^\circ$ and 108.4° , respectively.

3.3 Rotational constants from ground state averages (GSA)

For semi-rigid molecules, rotational and vibrational degrees of freedom can be treated in a Born-Oppenheimer approximation in which the Hamiltonian is averaged over the rotational ground state. This is achieved by defining an effective rotational Hamiltonian $H_{\text{rot}}^{\text{eff}}$

$$H_{\text{rot}}^{\text{eff}} = \sum_{i,j} \langle \Psi_0 | (I'^{-1})_{i,j} | \Psi_0 \rangle \hat{J}_i \hat{J}_j \quad (5)$$

where $I'_{i,j}$ are components of the effective inertial tensor (see Refs. [14,35]) calculated in the Eckart frame (x, y, z) . We use the definition of the Eckart frame axes given in Ref. [14], with interchange of y and z . Since for small

amplitude vibrations I' differs only slightly from the pure inertial tensor I , we have followed Ref. [14] and also calculated $\langle \Psi_0 | (I^{-1})_{i,j} | \Psi_0 \rangle$. For OCS-X, the effective rotational Hamiltonian (5) takes the form

$$H_{\text{rot}}^{\text{eff}} = A\hat{J}_x^2 + B\hat{J}_y^2 + C\hat{J}_z^2 + D(\hat{J}_x\hat{J}_y + \hat{J}_y\hat{J}_x) \quad (6)$$

where y is defined as the axis perpendicular to the OCS-X plane. The explicit expressions for A , B , C , and D are given in Ref. [14]. Rotational energies are then obtained by expanding $H_{\text{rot}}^{\text{eff}}$ in the symmetric rotor basis and diagonalizing the matrix. As noted already above in Section 2, we compute the exact ground state expectation values in Eq. (5) by descendant weighting of the importance sampling, in order to remove the trial wave function bias.

By an *ad hoc* combination of ccQA and GSA, one can also calculate rotational constants from (approximate) excited state averages in a similar fashion and use these to go back and calculate rotational energies. The procedure is as follows. First, sample an approximate excited state corresponding to (J, τ) defined by the effective Hamiltonian Eq. (4) of the ccQA approach explained in section 3.1. Second, calculate the rotational constants A , B , C , D as averages over these approximate excited states, *i.e.*, $\langle \Psi_{J,\tau} | \hat{A} | \Psi_{J,\tau} \rangle$ etc. This needs to be done also with descendant weighting to correct for the trial function bias. Third, diagonalize $H_{\text{rot}}^{\text{eff}}$ to obtain an updated estimate of the excitation energy $E_{J,\tau}$. We found that this *ad hoc* estimate turned out to be inferior to the ccQA results for both complexes, OCS-(H₂) and OCS-⁴He.

4 Results

We have applied the DMC-based approximate methods described above to the calculation of rotational excitation energies and rotational constants for OCS-(H₂) and OCS-⁴He and compared with the exact energies which we have determined using the program BOUND [15]. To relate the exact reference energies to rotational constants, we fitted the BOUND rotational energies to the eigenenergies of the Watson A-reduced Hamiltonian.[36] In case of the GSA calculation, the resulting rotational parameters A , B , C , D are used to construct the effective Hamiltonian (6) which we then diagonalized to obtain rotational energies.

In all calculations reported here, the imaginary time step value in the DMC walk was $dt/\hbar = 0.00011\text{cm}$ for OCS-(H₂) and $dt/\hbar = 0.00022\text{cm}$ for OCS-⁴He.

Fig. 2 shows the respective ground state densities of H₂ and ⁴He with respect to OCS, $\rho(r, \theta)$. These densities are obtained by simply binning the coordinates of

H_2 and ^4He in the body fixed frame of OCS in an unbiased DMC calculation, *i.e.* with trial function $\Phi_T = 1$, and then squaring the amplitude. The densities are qualitatively quite similar for the two complexes, with the helium density being somewhat more delocalized. In particular, we note that ^4He has a non-negligible probability to reside near the south pole of OCS (the oxygen end, at negative z). This leads us to expect that a semi-rigid approximation for $\text{OCS-}^4\text{He}$ might be problematic.

4.1 Exact excitation energies from BOUND

Fig. 3 summarizes the exact and quasi-adiabatic energy levels for OCS complexed with H_2 (top panel), and for OCS complexed with ^4He (middle and bottom panels). The exact energy levels are shown as horizontal bars. For the helium complex, we show the results from two different OCS-He potentials, namely the MP4 potential of Higgins and Klemperer [6] (middle panel) and the HHDS potential of Gianturco and Paesani [24] (bottom panel). The ground state energy of OCS-H_2 is -74.59 cm^{-1} and of $\text{OCS-}^4\text{He}$ is -16.38 cm^{-1} (MP4) / -15.85 cm^{-1} (HHDS). The exact results for OCS-H_2 show a very well-defined energetic separation between the low energy rotational states and the higher energy states associated with the vibrational motion of the H_2 molecule in the OCS-H_2 potential. For low values of J , the total angular momentum, these two different sets of states are separated by $\sim 25 \text{ cm}^{-1}$. This separation decreases as J increases and the rovibrational and purely rotational states are expected to mix, but even for $J = 6$, the highest value shown here, there is still a clear separation of $\sim 5 \text{ cm}^{-1}$ between the highest rotational sublevel and the first rovibrational level.

These results indicate that OCS-H_2 can be described as a rigid rotor and suggests that dynamic approximations based on such an assumption will provide a good starting point for *e.g.*, analyzing energy levels in larger clusters. This situation changes considerably for the lighter OCS-He complex. With both the MP4 potential (middle) and even more so with the HHDS potential (bottom) we find the energy separation between rotational and vibration levels greatly reduced. For small J , this separation is only $\sim 8 \text{ cm}^{-1}$ with the MP4 potential, and further decreases to $\sim 4 \text{ cm}^{-1}$ with the HHDS potential. This smaller separation between the purely rotational and rovibrational levels for the helium complex can be ascribed to the weaker interaction between OCS and ^4He .

The energetic spread of the rotational sublevels τ is also different between the two systems, with the helium complex levels being compressed relative to the corresponding levels in the hydrogen complex levels: the lighter mass of H_2 results in a large rotational constant A compared to B and C , which leads

to a steeper increase of the rotational energy with increasing $\tau = K_a - K_c$, *i.e.* for large K_a , which approximately corresponds to the fast rotation of H_2 about a tumbling OCS.

However, this smaller spread for the helium complex is clearly outweighed by the decrease in rovibrational energies. As a result of the smaller gap between rotational and rovibrational energies for OCS-He, a mixing of rotational and rovibrational levels is predicted at $J \geq 4$ for the HHDSD potential (bottom panel), and at $J \geq 5$ for the MP4 potential (middle panel). In comparison, for the OCS- H_2 complex the mixing does not occur until $J = 7$. The onset of this mixing of rovibrational and rotational levels at small J values is another indicator of non-rigid, “floppy”, behavior, seen here in the extreme for the helium complex. Therefore, from energy consideration, pure rotations cannot be distinguished from rovibrations at large values of the total angular quantum number J .

Table 3 and 4 list the parameters of the Watson A-reduced Hamiltonian obtained by fitting the energy levels obtained from the BOUND calculations to the following Watson A-reduced form:

$$\begin{aligned}
H_A = & \frac{1}{2}(B + C)\mathbf{J}^2 + [A - \frac{1}{2}(B + C)]\mathbf{J}_a^2 + \frac{1}{2}(B - C)(\mathbf{J}_b^2 - \mathbf{J}_c^2) - \Delta_J\mathbf{J}^4 \\
& - \Delta_{JK}\mathbf{J}_a^2\mathbf{J}^2 - \Delta_K\mathbf{J}_a^4 - 2\delta_J\mathbf{J}^2(\mathbf{J}_b^2 - \mathbf{J}_c^2) \\
& - \delta_K[\mathbf{J}_a^2(\mathbf{J}_b^2 - \mathbf{J}_c^2) + (\mathbf{J}_b^2 - \mathbf{J}_c^2)\mathbf{J}_a^2].
\end{aligned} \tag{7}$$

For comparison we show the corresponding experimental values of these parameters as determined spectroscopically in Refs. [7] and [8]. These were obtained by fitting to energy levels reaching up to $J = 6$, but still lying below the rovibrational levels. These tables provide a reference for the rotational constants derived from the approximate methods, described below, and provide a measure of the accuracy of the three potentials [6,23,24] considered in this work. Both complexes are fit by asymmetric top parameters.

4.2 Rotational energies from ccQA and Eckart modification (EccQA)

Both the assumption of separation of vibrational and rotational motion that is central to the ccQA approach, and the resulting effective Hamiltonian (5) break down when the respective vibrational and rotational energies are of similar magnitude. Thus from Fig. 3 and the discussion of the exact energies above, it appears that ccQA approach should break down at $J \sim 4 - 5$ for the helium complex, and at $J \sim 7$ for the hydrogen complex. The GSA calculation is also expected to fail at these J values. Furthermore, neither of these approaches can yield the higher rovibrational states, where, in addition

to the rotation of the complex, the H_2 or ^4He atom also vibrates radially with respect to the OCS molecule. To obtain estimates for the energies of these excited states possessing both vibrational and rotational character, one would need to sample the various excited vibrational states for $J = 0$ (*e.g.*, by imposing nodal constraints on the trial wave function [37,12], and then add the centrifugal potential $V_{J,\tau}(\mathbf{R})$ to the Hamiltonian (1) as described above to obtain vibrationally excited states with $J > 0$. Since this would introduce more approximations, we refrained here from trying to obtain the rovibrational excitation energies with ccQA beyond the pure rotational energies.

The ccQA energies for OCS- H_2 and OCS-He are shown as crosses in Fig. 3. They generally track the corresponding asymmetric top rotational energy levels, showing the greatest accuracy for the more rigid OCS- H_2 complex, and larger deviations for the more floppy OCS-He complex. For comparison, we have plotted as a continuous dotted line the quadratic behavior of the energy levels of free OCS, *i.e.*, $BJ(J+1)$, with $B = 0.2028 \text{ cm}^{-1}$. [18] It is notable that while both complexes are asymmetric tops, the free molecule line does nevertheless track the lowest set of rotational levels for OCS- H_2 , while for OCS-He the lowest rotational levels lie considerably lower than the free molecule values. In Figs. 4a, 4b, and 5, we show the error of the ccQA and EccQA calculations of rotational levels with respect to the exact BOUND energies, $\Delta E_{J,\tau} = E_{J,\tau}(\text{EccQA}) - E_{J,\tau}(\text{BOUND})$, for values of J where pure rotational levels can still be identified. Not surprisingly, the errors introduced by the (E)ccQA approximation are larger for the less rigid OCS- ^4He complex, see the larger y scale in Fig. 5, relative to Fig. 4a. Nevertheless, the deviations of (E)ccQA from the exact energies are still quite small in both cases, considering that both dimers, especially OCS- ^4He , experience large zero-point motion (see Fig. 2). Comparing now the original quasi-adiabatic approach (ccQA, closed symbols in Figs. 4a, 4b, and 5) with the Eckart modification (EccQA, open symbols), we see that the introduction of the Eckart reference frame does not improve the accuracy of the results. For completeness, we also have compared the relative errors for OCS-He when the two different potentials are used, MP4 and HHDS (not shown). Since the HHDS interaction is less anisotropic, Fig. 1, and allows for larger zero-point motion of the ^4He atom, the (E)ccQA approximation yields poorer results with the HHDS interaction than with the MP4 interaction, by up to a factor of two for $J = 1 - 3$.

Fig. 6 shows the mean distance $\langle r \rangle$ of H_2 and ^4He , respectively, from OCS for the rotational excited states (J, τ) , obtained in the ccQA approximation. Although $\langle r \rangle$ spans a smaller range for OCS- H_2 due to the larger rigidity, $\langle r \rangle$ rises more steeply with $\tau = K_a - K_c$, because of the high energies involved with the quantum number K_a (see the comment above about the larger spread in energies evident in Fig. 3).

4.3 GSA

The four rotational parameters of the ground state effective Hamiltonian $H_{\text{rot}}^{\text{eff}}$, eq. (6), are tabulated in Table 5. Comparison with the fits to the exact energy levels shown in Tables 3 and 4 show that using the pure inertial tensor I instead of the effective inertial tensor I' tends to improve the agreement with the values of the asymmetric top rotational constants A, B, C from fitting to the BOUND results. We note that, other than for the ccQA approximation, GSA rotational constants are sensitive to the choice of axis system, and the Eckart conditions may not be neglected.

The deviations of the eigenenergies of $H_{\text{rot}}^{\text{eff}}$ from the exact rotational energies are shown in Figs. 7a, 7b, and 8 for OCS-(H₂) and OCS-⁴He, respectively. Comparison with Figs. 4a and 4b shows that, for OCS-H₂, the GSA deviations are of similar magnitude as those of the ccQA approximation, with GSA doing slightly better for smaller J than ccQA and vice versa for larger J . For OCS-⁴He, the deviations of GSA increase faster with J . Also, table 5 shows that, just like ccQA, GSA is less accurate for OCS-⁴He than for OCS-(H₂). There is a small, but finite probability for the ⁴He atom to be close to the oxygen side, along the OCS axis, *i.e.* OCS-⁴He vibrating end-over-end. For these configurations, the rotational constants A , $C(C')$, and D diverge, leading to poor statistics in the DMC calculation.

5 Conclusions

We have compared the exact rotational excitation energies of the weakly bound Van der Waals complexes OCS-paraH₂ and OCS-⁴He with two approximate methods, namely, the clamped coordinate quasiadiabatic approximation (ccQA) and ground state averages of the rotational constants (GSA), as well as with variants of each of these methods. The purpose of this survey is to assess which approximate methods will work best for larger complexes OCS-(H₂)_{*N*} and OCS-⁴He_{*N*}, in the absence of non-stochastic exact techniques.

While for the GSA approach, fulfilling the Eckart condition improves the results considerably, we found no significant improvement of the ccQA results when the instantaneous inertial frame is replaced by the Eckart frame (Ec-cQA). This is good news for larger size clusters, since incorporating the Eckart condition brings with it the need to define a reference structure, which would become increasingly cumbersome and less tractable for growing N . We also found that incorporation of a centrifugal correction in the instantaneous inertial matrix in the GSA method (Section 3.3) actually tends to degrade the accuracy of the excitation energies. This is in agreement with the findings of

Ref. [14].

A significant physical feature that emerged from comparison of the complete energy spectrum of rotational and rovibrational states for the two complexes of OCS with H_2 and with He, is the greater rigidity of the hydrogen complex, as evident from the larger separation between purely rotational and rovibrational states. This was evident from surveying the overall pattern of energy levels, Fig. 3. Experimental investigation of vibrationally excited states for OCS- H_2 and OCS- ^4He would be useful, because their energies are most sensitive to the potential surface $V(r, \cos \theta)$ at higher energies and larger r values. This differentiation in rigidity apparent from examination of the excited state spectrum is particularly interesting given the close similarity of the ground state densities for the two complexes (Fig. 2).

A detailed projection for the breakdown of the assumption of separability of vibrational and rotational excitations in the multi-particle complexes OCS- X_N , $N > 1$, is of course difficult, because exact results for *all* excited state energies are currently impossible to obtain for large N . However, the projection operator imaginary time spectral evolution approach (POITSE) can provide exact energies given a good trial wave function. It yields the energies of *selected* rotational states, where the selection is determined by the choice of a projector acting on the ground state. POITSE calculations [11] of rotational excitations of OCS- $^4\text{He}_N$ for $N \leq 20$ show approximate agreement with ccQA results for $N \leq 5$ and $J = 1$, with the ccQA results lying always somewhat lower than the POITSE results. This agreement with exact calculations indicates that the rigid coupling approximation underlying the ccQA approximation is good in this regime. For larger N , the POITSE rotational energy saturates in accordance with experimental results, while the energies obtained in ccQA and GSA monotonically decrease for increasing N . This implies that not all ^4He atoms in the first solvation shell can rigidly follow the OCS rotation, as discussed extensively in Ref. [19] and demonstrated explicitly in Ref. [11].

6 Acknowledgments

This work was supported by the NSF under grant CHE-0107541, and the Miller Institute for Basic Research in Science at the University of California, Berkeley. The authors would like to thank Francesco Paesani for providing the program to fit the rotational energies to the Watson A-reduced Hamiltonian, Patrick Huang for valuable discussions about correlated Monte Carlo sampling, and E. Krotscheck for providing computational resources of the Central Information Services of the Kepler University, Linz, Austria.

References

- [1] J. P. Toennies, A. F. Vilesov, K. B. Whaley, Superfluid helium droplets: an ultracold nanolaboratory, *Physics Today* 54 (2) (2001) 31.
- [2] J. P. Toennies, A. F. Vilesov, Spectroscopy of atoms and molecules in liquid helium, *Annu. Rev. Phys. Chem.* 49 (1998) 1.
- [3] S. Grebenev, J. P. Toennies, A. F. Vilesov, Superfluidity within a small helium-4 cluster: The microscopic andronikashvili experiment, *Science* 279 (1998) 2083.
- [4] S. Grebenev, B. Sartakov, J. P. Toennies, A. F. Vilesov, Evidence for superfluidity in para-hydrogen clusters inside helium-4 droplets at 0.15 kelvin, *Science* 289 (2000) 1532.
- [5] Y. Kwon, K. B. Whaley, Nanoscale molecular superfluidity of hydrogen, *Phys. Rev. Lett.* (2002) submitted.
- [6] K. Higgins, W. H. Klemperer, The intermolecular potential of He-OCS, *J. Chem. Phys.* 110 (3) (1999) 1383.
- [7] J. Tang, A. R. W. McKellar, Infrared spectrum of the OCS-He complex, *J. Chem. Phys.* 115 (7) (2001) 3053.
- [8] J. Tang, A. R. W. McKellar, Infrared spectrum of the OCS-hydrogen complex, *J. Chem. Phys.* 116 (2) (2002) 646.
- [9] Y. Xu, W. Jäger, Fourier transform microwave spectroscopic investigation of a very weakly bound ternary complex: OCS-He₂, *Chem. Phys. Lett.* 350 (2001) 417.
- [10] J. Tang, Y. Xu, A. R. W. McKellar, W. Jäger, Quantum solvation of carbonyl sulfide with helium atoms, *Science* 297 (2002) 2030.
- [11] F. Paesani, A. Viel, F. A. Gianturco, K. B. Whaley, Transition from molecular complex to quantum solvation in ⁴He_NOCS, submitted to *Phys. Rev. Lett.* (2002).
- [12] M. Quack, M. A. Suhm, Potential energy surfaces, quasiadiabatic channels, rovibrational spectra, and intramolecular dynamics of (HF)₂ and its isotopomers from quantum Monte Carlo calculations, *J. Chem. Phys.* 95 (1) (1991) 28.
- [13] C. Eckart, Some studies concerning rotating axes and polyatomic molecules, *Phys. Rev.* 47 (1935) 552.
- [14] A. Ernesti, J. M. Hutson, On the rotational constants of floppy molecules, *Chem. Phys. Lett.* 222 (1994) 257.
- [15] J. M. Hutson, Bound computer code, version 5, distributed by Collaborative Computational Project No. 6 of the Science and Engineering Research Council (UK) (1993).

- [16] R. C. Cohen, R. J. Saykally, Multidimensional intermolecular dynamics from tunable far-infrared laser spectroscopy: Angular-radial coupling in the intermolecular potential of argon-H₂, *J. Chem. Phys.* 95 (1991) 7891.
- [17] C. Leforestier, Grid method for the wigner functions. application to the van der waals system ar-ho₂, *J. Chem. Phys.* 101 (1994) 7357.
- [18] S. Grebenev, M. Hartmann, M. Havenith, B. Sartakov, J. P. Toennies, A. F. Vilesov, The rotational spectrum of single ocs in liquid ⁴He droplets, *J. Chem. Phys.* 112 (10) (2000) 4485.
- [19] Y. Kwon, P. Huang, M. V. Patel, D. Blume, K. B. Whaley, Molecular rotations in superfluid helium clusters, *J. Chem. Phys.* 113 (2000) 6469–6501.
- [20] R. Guardiola, Monte Carlo methods in quantum many-body theories, in: J. Navarro, A. Polls (Eds.), *Microscopic Quantum Many-Body Theories and Their Applications*, Vol. 510 of *Lecture Notes in Physics*, Springer, 1998, pp. 269–336.
- [21] B. L. Hammond, W. A. L. Jr., P. J. Reynolds, *Monte Carlo methods in ab initio quantum chemistry*, World Scientific, 1994.
- [22] C. J. Umrigar, M. P. Nightingale, K. J. Runge, A diffusion Monte Carlo algorithm with very small time-step error, *J. Chem. Phys.* 99 (4) (1993) 2865.
- [23] K. Higgins, Z. Yu, W. H. Klemperer, to be published (2002).
- [24] F. A. Gianturco, F. Paesani, The He-OCS van der Waals potential from model calculations: Bound states, stable structures, and vibrational couplings, *J. Chem. Phys.* 113 (8) (2000) 3011.
- [25] J. M. M. Howson, J. M. Hutson, Morphing the He-OCS intermolecular potential, *J. Chem. Phys.* 115 (11) (2001) 5059.
- [26] V. Buch, *J. Chem. Phys.* 97 (1992) 726.
- [27] A. Viel, M. V. Patel, P. Niyaz, K. B. Whaley, Importance sampling in rigid body diffusion Monte Carlo, *Comp. Phys. Comm.* 145 (2002) 24–47.
- [28] K. S. Liu, M. H. Kalos, G. V. Chester, *Phys. Rev. A* 10 (1974) 303.
- [29] J. Casulleras, J. Boronat, Unbiased estimators in quantum Monte Carlo methods: Application to liquid ⁴He, *Phys. Rev. B* 52 (5) (1995) 3654.
- [30] D. Blume, M. Lewerenz, P. Niyaz, K. B. Whaley, Excited states by quantum Monte Carlo methods: Imaginary time evolution with projection operators 55 (3) (1997) 3664.
- [31] A. Viel, K. B. Whaley, Quantum structure and rotational dynamics of HCN in helium droplets, *J. Chem. Phys.* 115 (22) (2001) 10186.
- [32] R. N. Zare, *Angular Momentum*, Wiley Interscience, New York, 1988.
- [33] B. H. Wells, The differential Green’s function Monte Carlo method. the dipole moment of LiH, *Chem. Phys. Lett.* 115 (1) (1985) 89.

- [34] M. Schinnacher, Methoden zur quantenmechanischen simulation von dotierten van der waals clustern Ar_NCl und Ar_NHF , Master's thesis, Univ. Göttingen (1996).
- [35] E. B. Wilson, J. C. Decius, P. C. Cross, Molecular Vibrations, Dover, 1980.
- [36] P. R. Bunker, P. Jensen, Molecular Symmetry and Spectroscopy, 2nd Edition, NRC Research Press, 1998.
- [37] M. Lewerenz, Quantum Monte Carlo calculation of argon-HF clusters: Nonadditive forces, isomerization, and HF frequency shifts, J. Chem. Phys. 104 (1996) 1028–1039.

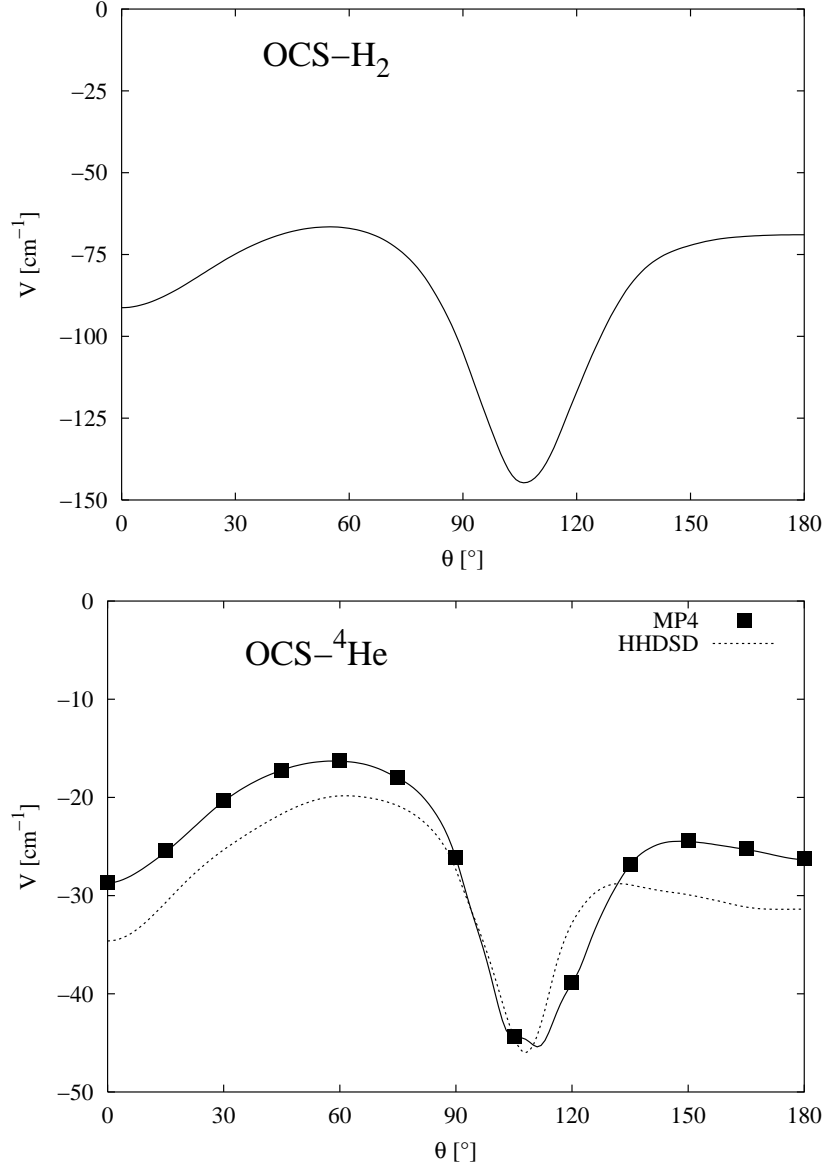


Fig. 1. The interaction energy along the minimum energy path of the potential energy surface $V(r, \cos \theta)$ between H₂ and OCS (top) [23] and ⁴He and OCS (bottom). For the latter we show both potentials used in our calculations, MP4 by Higgins *et.al.* [6] (squares are *ab initio* points from that reference) and HHDS by Gianturco *et.al.* [24] (dashed line). For usage in the DMC simulations, all potentials have been interpolated from the *ab initio* data points by splines in radial direction and by expansion in Legendre polynomials in angular direction, see Ref. [24].

Table 1

Parameters for the trial wave function (2) where r is in Å.

	a_1	α	t_1	η_1	u_1	a_2	t_2	η_2	u_2	η	c
OCS-(H ₂)	-6.6	0.79	6.4	-1.28	-0.22	0.529	-1.0	-0.71	-0.22	5.9	1.59
OCS- ⁴ He	-5.9	0.79	7.68	-0.32	0.0	0.529	-1.0	-0.57	-0.26	6.3	1.78

Table 2

Equilibrium configuration and root mean square deviations.

	$\langle r \rangle [\text{\AA}]$	$\langle \cos \theta \rangle$	$\Delta r [\text{\AA}]$	$\Delta \cos \theta$
OCS-(H ₂)	3.704	-0.270	0.364	0.158
OCS- ⁴ He	3.935	-0.315	0.478	0.200

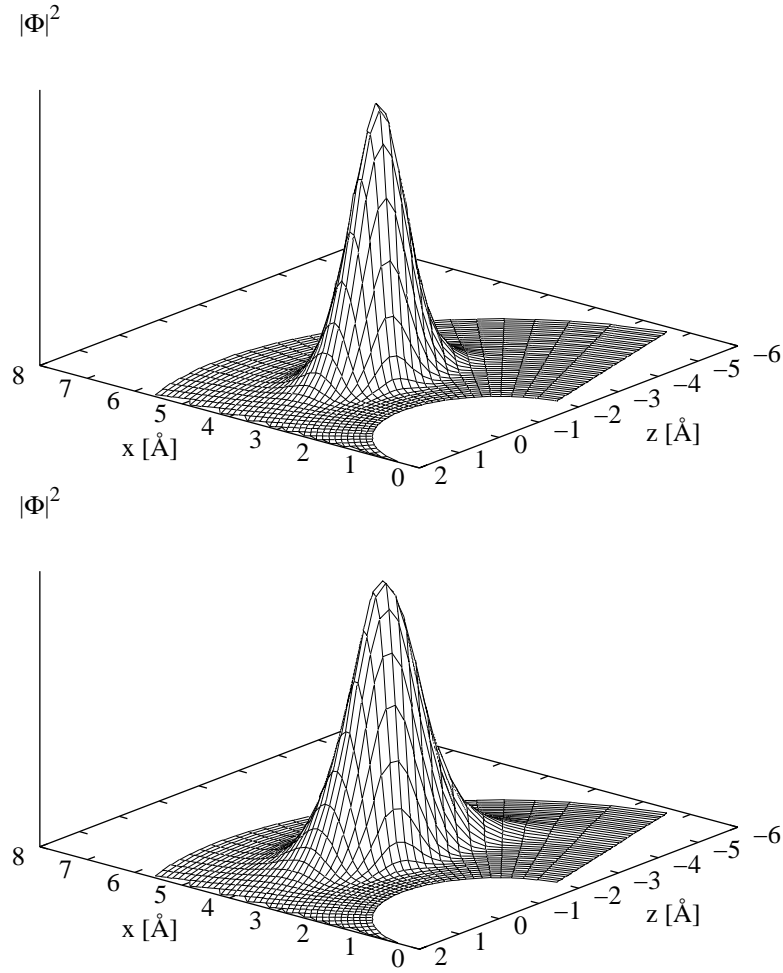


Fig. 2. Probability density $\rho(r, \theta)$ for H_2 (top) and ^4He (MP4 potential of Higgins *et.al.* [6], bottom) to be found at distance r from the OCS center of mass and at angle θ in the OCS fixed coordinate system, obtained from unbiased DMC. The OCS molecule is oriented along the z -axis, with oxygen at negative z , and the x -axis is defined as any axis perpendicular to z .

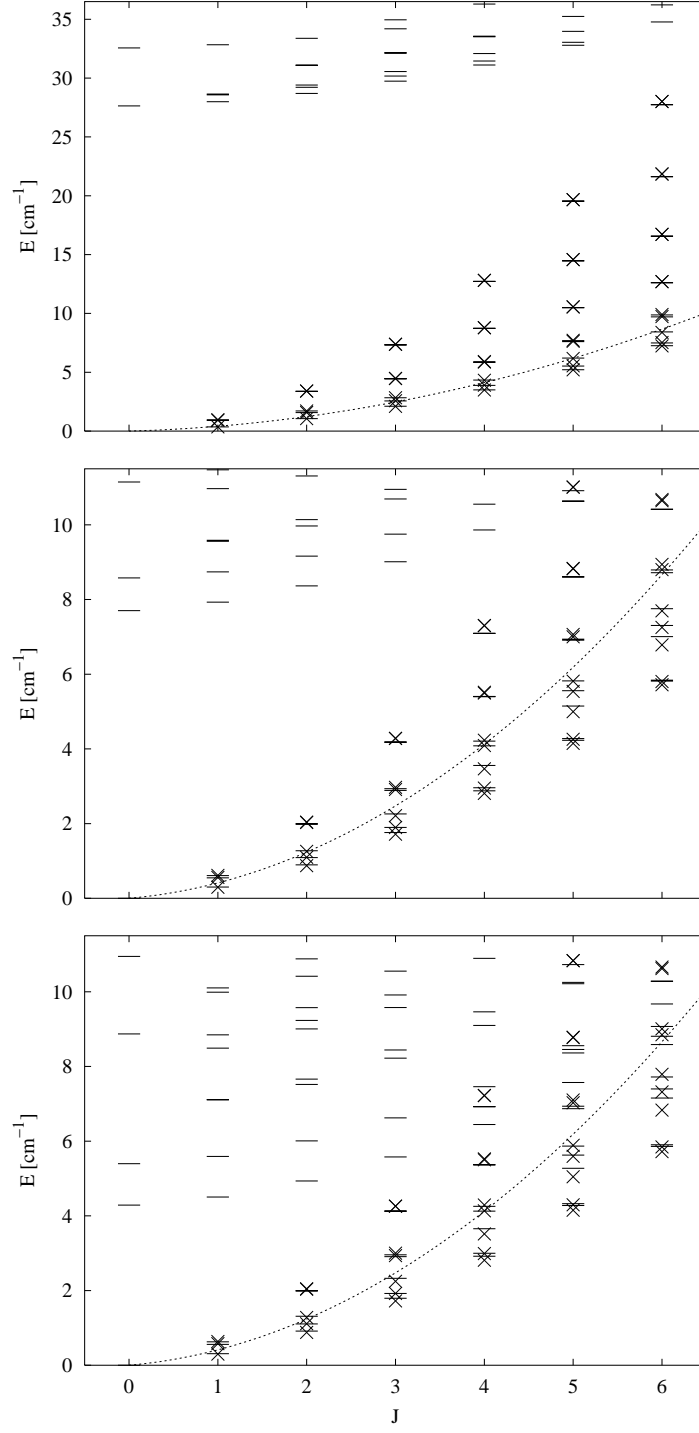


Fig. 3. Top panel: excitation energies $E_{J,i}$ of OCS-(H₂), obtained by BOUND and in the clamped coordinate quasi-adiabatic approximation; middle and bottom panels: $E_{J,i}$ for OCS-⁴He, using the MP4 potential of Higgins *et.al.* [6] (middle) and the HHDS potential of [24] (bottom). For comparison, the dotted line shows the quadratic behavior of the free OCS rotational energy levels $B J(J+1)$, with $B = 0.2028 \text{ cm}^{-1}$. [18]

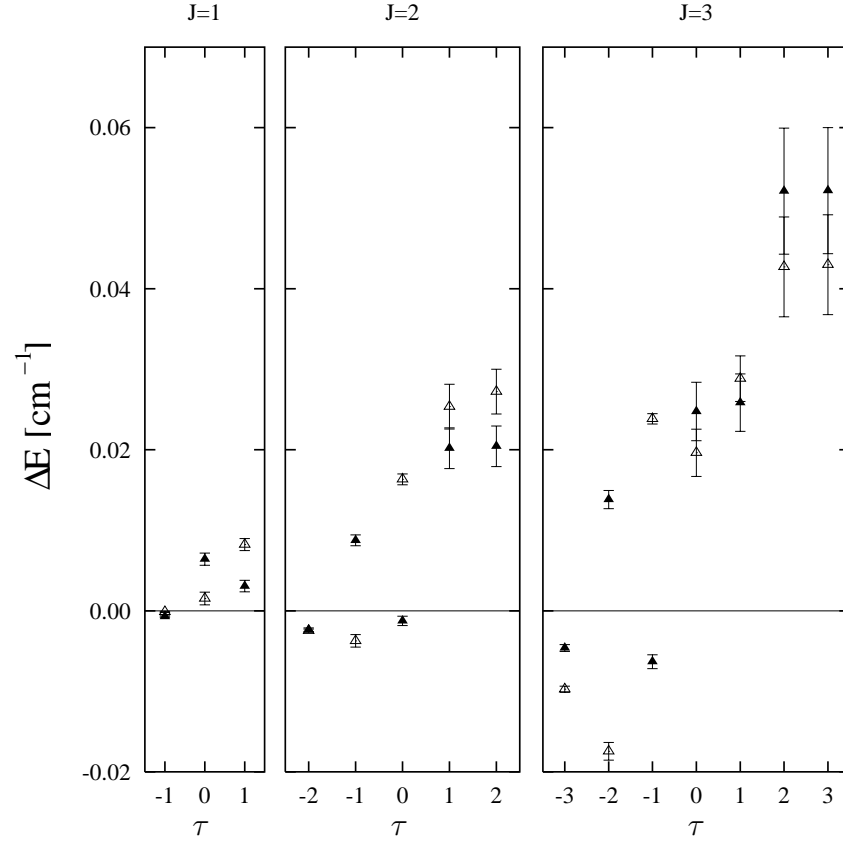


Fig. 4a. The error made in ccQA (filled triangles) and EccQA (open triangles), $\Delta E_{J,\tau} = E_{J,\tau}(\text{EccQA}) - E_{J,\tau}(\text{BOUND})$, for the complex of OCS with hydrogen, OCS-H_2 , $J = 1, 2, 3$.

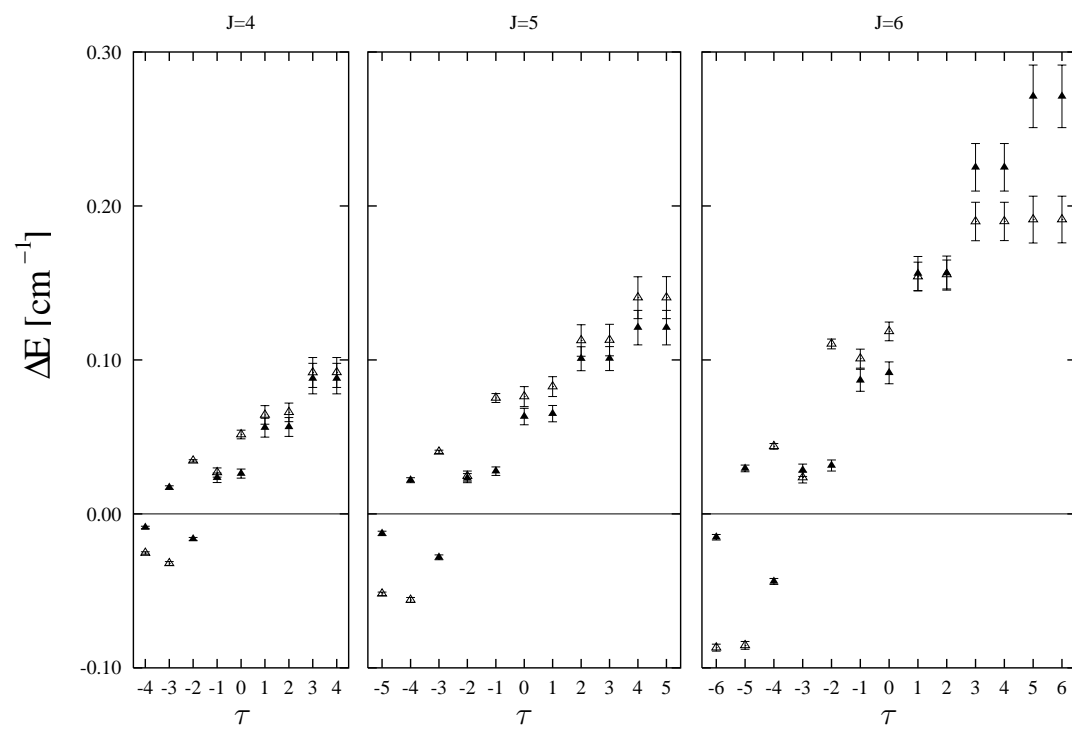


Fig. 4b. Same as Fig. 4a for $J = 4, 5, 6$.

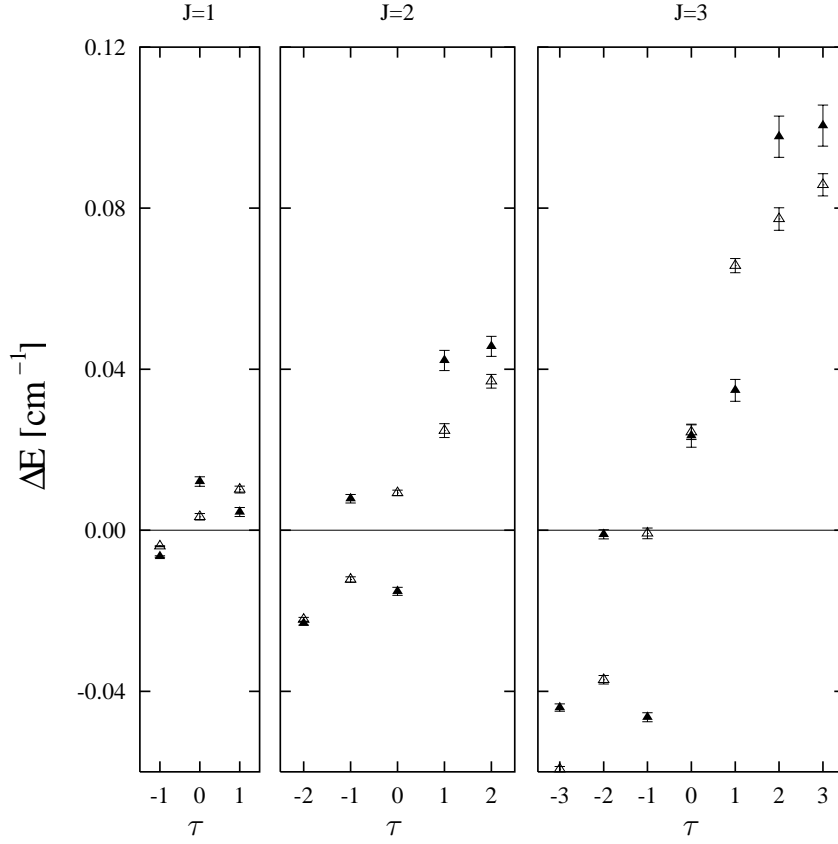


Fig. 5. The error made in ccQA (filled triangles) and EccQA (open triangles), $\Delta E_{J,\tau} = E_{J,\tau}((E)\text{ccQA}) - E_{J,\tau}(\text{BOUND})$, for the complex of OCS with helium, $\text{OCS-}^4\text{He}$, $J = 1, 2, 3$, using the MP4 potential of Higgins *et.al.* [6]. Note the larger vertical scale, relative to that for $\text{OCS-(H}_2\text{)}$ in Fig. 4a.

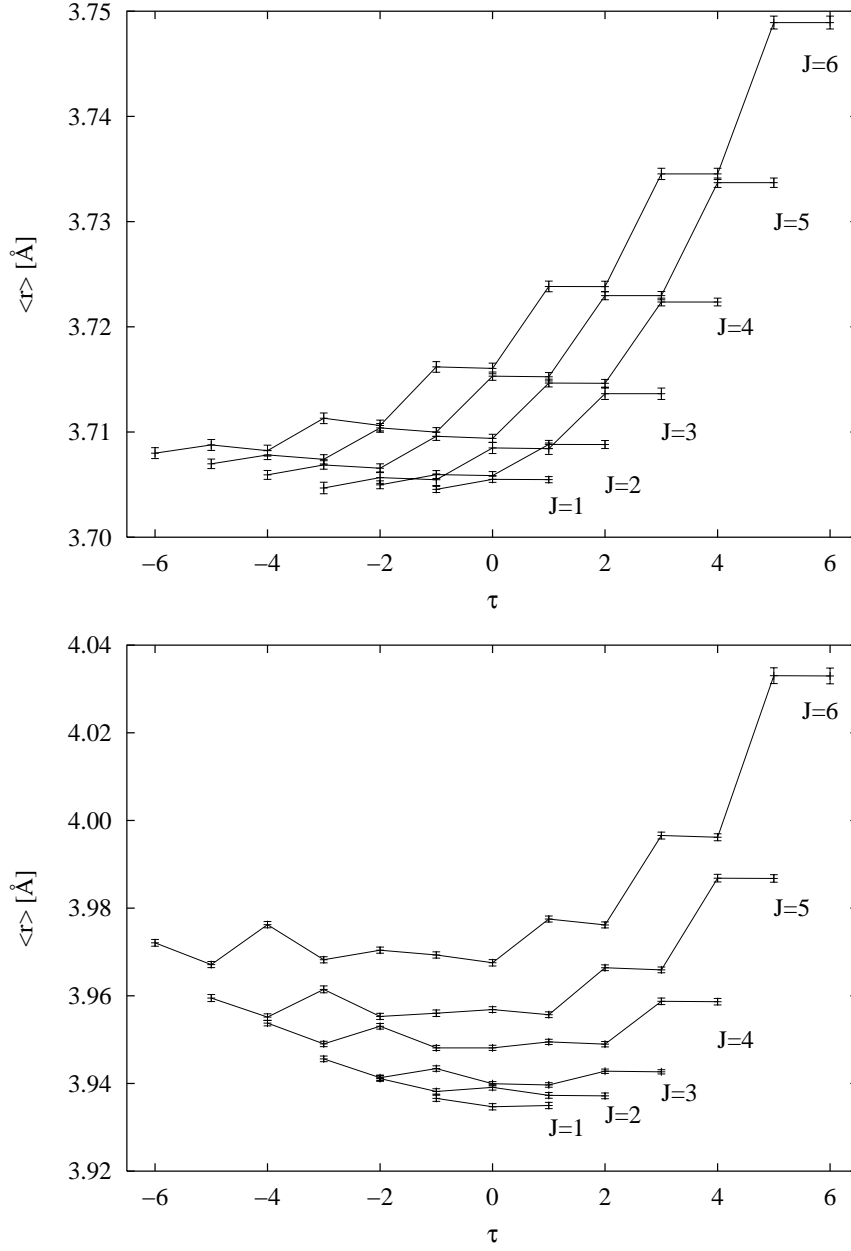


Fig. 6. Mean distance $\langle r \rangle$ between H₂ (top) and ⁴He (MP4 potential of Higgins *et.al.* [6], bottom), respectively, and the center of mass of OCS, for $J = 0, \dots, 6$ and $\tau = -J, \dots, J$, in ccQA approximation.

Table 3

Parameters of the Watson A-reduced Hamiltonian, eq. 7, for OCS-(H₂) by fitting to the energies obtained by BOUND, $J = 1, \dots, 6$, and to the experimental energies of Ref. [8].

	MP4	exp.[8]
A	0.7595	0.7607
B	0.1997	0.19996
C	0.1540	0.15344
Δ_J	1.4×10^{-6}	2.4×10^{-6}
Δ_{JK}	1.7×10^{-4}	1.56×10^{-4}
Δ_K	3.1×10^{-4}	10^{-3}
δ_J	3.7×10^{-7}	7×10^{-7}
δ_K	1.23×10^{-4}	1.4×10^{-4}

Table 4

Parameters of the Watson A-reduced Hamiltonian, eq. 7, for OCS-⁴He by fitting to the energies obtained by BOUND, $J = 1, \dots, 4$, for both, the MP4 and the HHDSO potential, and to the experimental energies of Ref. [7].

	MP4	HHDSO	exp.[7]
A	0.4253	0.4309	0.44059
B	0.1833	0.1946	0.1835992
C	0.1198	0.1191	0.1221314
Δ_J	6.260×10^{-5}	2.244×10^{-4}	3.1378×10^{-5}
Δ_{JK}	-5.40×10^{-5}	-8.40×10^{-5}	4.669×10^{-5}
Δ_K	1.23×10^{-3}	2.50×10^{-3}	1.43663×10^{-3}
δ_J	1.89×10^{-5}	3.42×10^{-5}	1.12265×10^{-5}
δ_K	4.38×10^{-4}	1.55×10^{-4}	3.2667×10^{-4}

Table 5

Parameters of the effective Hamiltonian $H_{\text{rot}}^{\text{eff}}$, eq. (6), for OCS-H₂ and OCS-⁴He (MP4 potential of Higgins *et.al.* [6]),

	OCS-(H ₂) [cm ⁻¹]	OCS- ⁴ He [cm ⁻¹]
A	0.7520(2)	0.42(3)
B	0.20318(5)	0.206(8)
C	0.15556(7)	0.12084(2)
C'	0.15663(5)	0.13355(3)
D	0.0016(6)	-0.07(2)

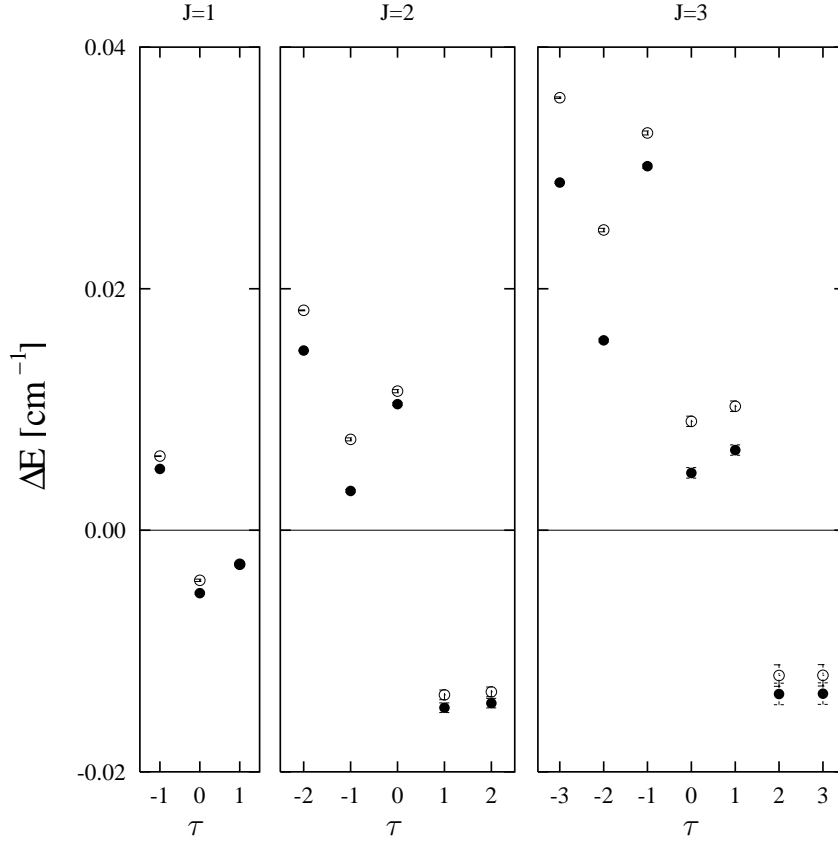


Fig. 7a. The error made in the ground state average calculation, $\Delta E_{J,\tau} = E_{J,\tau}(\text{GSA}) - E_{J,\tau}(\text{BOUND})$, for the complex of OCS with hydrogen, OCS-(H₂), $J = 1, 2, 3$. Both inertial matrices, I (filled circles) and I' (open circles), were used.

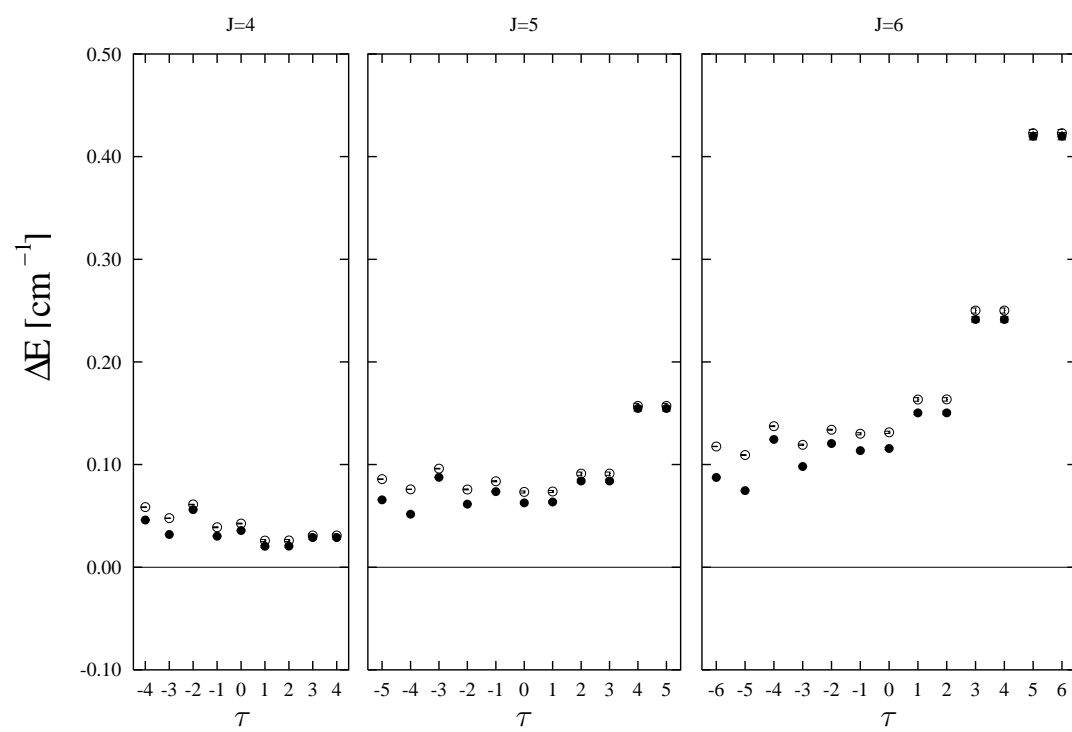


Fig. 7b. Same as Fig. 7a for $J = 4, 5, 6$.

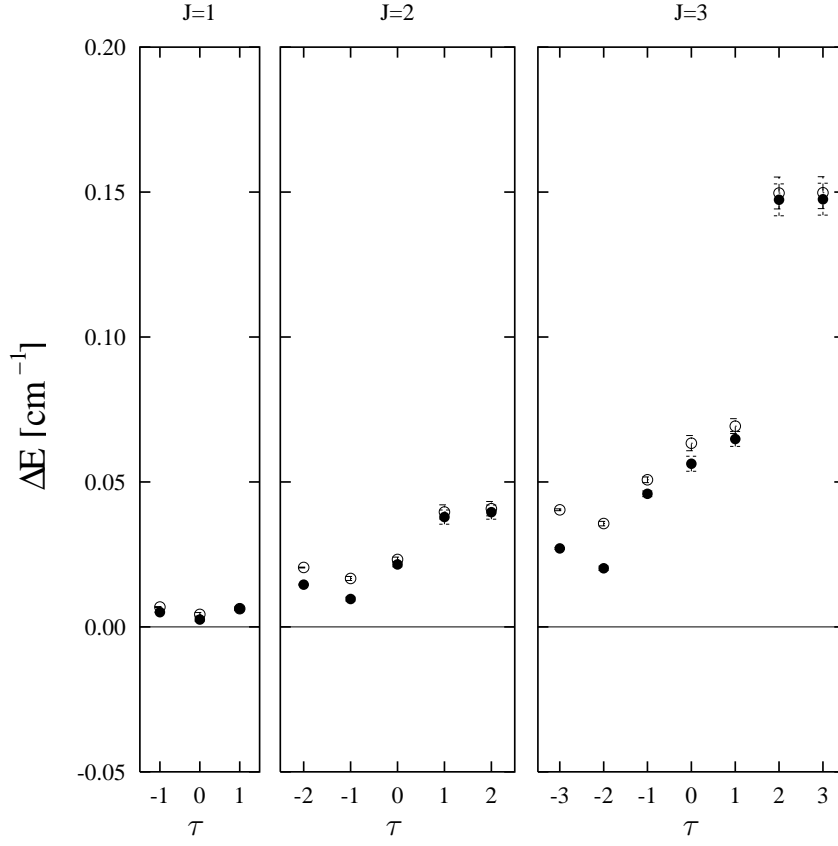


Fig. 8. The error made in the ground state average calculation, $\Delta E_{J,\tau} = E_{J,\tau}(\text{GSA}) - E_{J,\tau}(\text{BOUND})$, for the complex of OCS with helium, $\text{OCS-}^4\text{He}$, $J = 1, 2, 3$ (MP4 potential of Higgins *et.al.* [6]). Both inertial matrices, I (filled) and I' (open), were used.